Check for updates

Received: 24 May 2022 | Accepted: 6 August 2022

DOI: 10.1111/ffe.13812

SPECIAL ISSUE ARTICLE

FFEMS Fatigue & Fracture of Engineering Materials & Structures WILEY

Actual weld profile fatigue performance by digital prototyping of defected and un-defected joints

Paolo Livieri | **Roberto Tovo**

Department of Engineering, University of Ferrara, Ferrara, Italy

Correspondence
Paolo Livieri, Department of Engineering, University of Ferrara, via Saragat 1, 44122 Ferrara, Italy.
Email: paolo.livieri@unife.it

Abstract

This paper considers the effects of the actual weld profile on the fatigue behavior of welded joints by means of the implicit gradient approach. Different types of geometrical approximation are considered in the analysis. In order to define the fatigue strength reduction factor of the actual weld profile, FE analyses have been considered based on a three-dimensional scan of the welded joints. Furthermore, the fatigue behavior of butt-welded joints with a discontinuous undercut is considered, and a comparison has been made with experimental data taken from the literature.

KEYWORDS

defects, fatigue, implicit gradient, welded joints

1 | INTRODUCTION

Defects could be present in welded joints, and their shape and size acceptability levels have to be checked in documents such as ISO 6520 *Classification of imperfections in metallic fusion welds*,[1] ISO 5817,[2] and ISO 10042.[3] In general, the shape of the defects is evaluated in a basic manner, and some general limitations are given on the size and position of the flaw. From a schematic point of view, the defects can be classified as imperfect shapes (linear misalignment and angular distortions), undercuts, volumetric discontinuities (gas pore and cavities of any shape), and planar discontinuities (lack of fusion or lack of penetration) as is the case, for instance, by Hobbacher.[4] Schork et al.[5] suggested the use of the FAT class in conjunction with the ISO quality system. For instance, the Volvo Standard STD 181-0004[6] proposes eight parameters to assess the reduction in fatigue performance of defected joints. When classifying defects, the definition of the defect reference shape and its critical dimensions is a challenging task; for instance, concerning undercuts, the depth compared to the plate thickness is considered in the above-mentioned document, but there is no definition or consideration concerning its actual overall shape. In the literature, an ideal V-rounded notch or semi-circular notch are commonly considered as the reference theoretical shape for both analytical or numerical studies.[4,7] Alternatively, by considering the development of weld quality criteria based on fatigue performance, Jonsson et al. provide a weld quality guideline which quantitatively relates weld acceptance criteria to the expected structural performance.[8]

Conversely, it is possible by means of 3D scanners to easily digitize any object, by addressing its actual shape, without any assumption or conjecture on the reference or theoretical defect shape. 3D scanners allow the researcher to easily acquire even complex geometries and offer the absolute rendering of particular textures. Superficial defects at the weld toe can be reproduced exactly in a virtual model without introducing simplifications, modifications, or assumptions. Generally, from a three-dimensional scan, it is possible to obtain an accurate graphical representation of the weld toe radius, weld toe flank angle, undercut depth, weld reinforcement size, primary and secondary notch depth, and so on.[5]

Obviously, these specific geometrical parameters are taken from one or several samples, and usually, the welding process has a considerable variability, so that the

 © 2022 John Wiley & Sons Ltd.

average values, scatters, variance, or other statistical property are considered.

As far as a specific joint geometry is known or assumed, the implicit gradient approach proposed in Livieri and Tovo[9] could also be useful for a numerical analysis of the fatigue performance of welded joints with defects such as undercuts, pores, misalignments, and so on because it considers the actual geometry of the weld profile without simplifying or adding a crack. Actually, the problem of the fatigue strength assessment of underflushing by excessive grinding on the weld throat has been addressed through the implicit gradient approach and has been verified by a set of experimental tests.[10] The implicit gradient approach is particularly suitable for analyzing welded joints as three-dimensional structures without introducing geometrical simplification since the Cauchy stress field singularity is transformed into a continuous equivalent stress field. Furthermore, if a three-dimensional laser scanning of the weld is available, an accurate 3D model could be considered and the numerical analysis could give the exact point of the fatigue crack initiation. Alternatively, by means of linear fracture mechanics, the defects can be considered as an elliptical or semi elliptical crack,[11,12] and then, the propagation of the flaw can be considered according to the linear elastic fracture.[13–15]

This paper examines the problem of three-dimensional defects in welded joints by means of the implicit gradient approach. In particular, the undercuts problem is considered an example of the systematic analysis of the weld toe in complex structures. Then, in order to provide the capability of the implicit gradient approach in considering the effect of the undercut at the weld toe, the fatigue behavior of the steel butt-welded joint has been evaluated. Finally, an FE analysis of a butt-welded joint based on an accurate three-dimension scan of the joint is proposed. This paper, and the related methodology, only tackle the effect of the overall geometry on fatigue strength, assuming that other conditions at the weldment can be considered substantially constant, as well as the metallurgical features, residual stress, or other defects that have not been explicitly considered. This assumption has been commented in Livieri and Tovo[10] where it has been substantially proved that this is suitable for fatigue assessment of defected welded joints.

1.1 | The implicit gradient approach

In previous papers,[16,17] the authors proposed the use of the implicit gradient approach as an engineering tool for the definition of effective stress obtained directly from FE analysis. This approach considers the effective stress σ_{eff}, which is calculated numerically by means of two consecutive FE analysis, as critical for the material. The first is the usual FE analysis for the assessments of the Cauchy stress by considering the material as linear elastic or elasto-plastic.[18] The second analysis is performed with the scope of solving the Helmholtz differential equation in volume V of the component by imposing the Neumann boundary conditions[19]:

$$\sigma_{eff} - c^2 \nabla^2 \sigma_{eff} = \sigma_{eq} \quad in \quad V \tag{1}$$

In Equation 1, the known term is the equivalent stress σ_{eq} obtained from previous FE analysis (for welded joints under proportional loading σ_{eq} agrees with the maximum principal stress σ_1). ∇^2 is the Laplace operator, and Neuman boundary conditions are assumed: $\nabla\sigma_{eff} \cdot n = 0$ (where $\nabla\sigma_{eff}$ is the gradient of the effective stress and n the outward normal vector). The characteristic length of the material, which characterizes all local approaches,[20] occurs in the c parameter. For welded joints made of steel, a value of 0.2 mm appears to be a reasonable value that is able to resume the fatigue strength of many different types of welded joints subjected to tensile or bending loading[16] whereas c is equal to 0.15 for aluminum-welded joints.[17] In all FE analyses reported in this paper, c was always considered equal to 0.2 mm as well as E = 207 GPa and ν = 0.3. The evaluation of the effective stress σ_{eff} gives us the position of the initiation fatigue crack and the capability of evaluating the fatigue life by means of a master fatigue curve that does not depend on the load, shape, and size of the weld but only on the material.

From a physical point of view, Equation (1) is an alternative form to evaluate the average of σ_{eq} inside volume V of the component according to the non-local theory as proposed by G. Pijaudier-Cabot and Z. P. Bažant[21,22]:

$$\sigma_{av}(P) = \frac{\int_V \Psi(P,Q)\,\sigma_{eq}(Q)\,dV}{\int_V \Psi(P,Q)\,dV} \tag{2}$$

where $\psi(P,Q)$ denotes a homogeneous isotropic weight function, such as the Gaussian function, of the distance $\|P-Q\|$ between the actual point $\boldsymbol{P}$ and the generic point $\boldsymbol{Q}$ of volume V. In this scenario, the effective stress σ_{eff} given by Equation 1 is an efficient tool to evaluate in each point $\boldsymbol{P}$ of volume V the average stress σ_{av}, and if a Gaussian weight function ψ (**x**,**y**) is assumed, it is possible to show that c is related to the mean root of the weight function.[23–25] The use of the weight function

14602695, 2022, 11, Downloaded from https://onlinelibrary.wiley.com/doi/10.1111/ffe.13812 by Universita Di Ferrara, Wiley Online Library on [20/06/2024]. See the Terms and Conditions (https://onlinelibrary.wiley.com/terms-and-conditions) on Wiley Online Library for rules of use; OA articles are governed by the applicable Creative Commons License

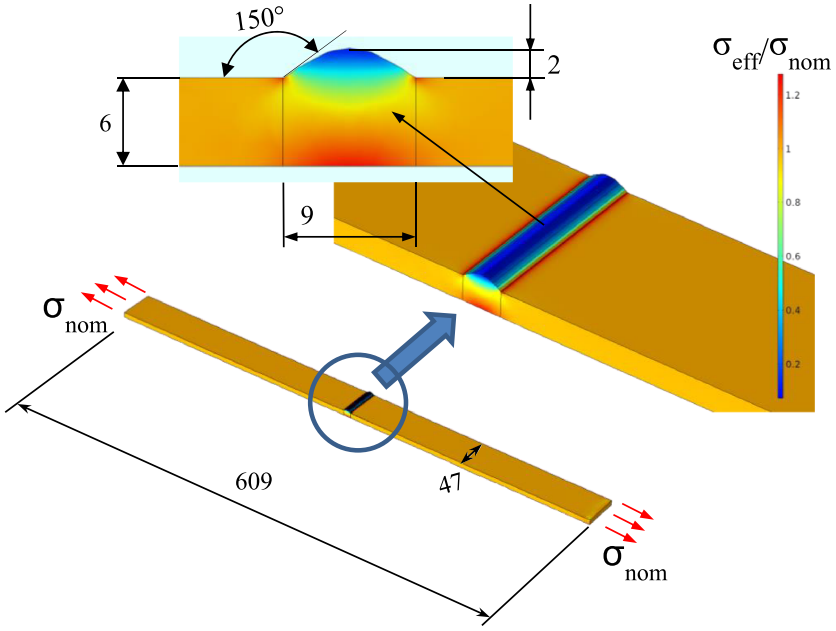

FIGURE 1 Effective stress σeff in dimensionless form for a butt-welded joint under axial loading σ_{nom} (dimension in millimeters; $c = 0.2$ mm; weld toe radius equal to zero) [Colour figure can be viewed at wileyonlinelibrary.com]

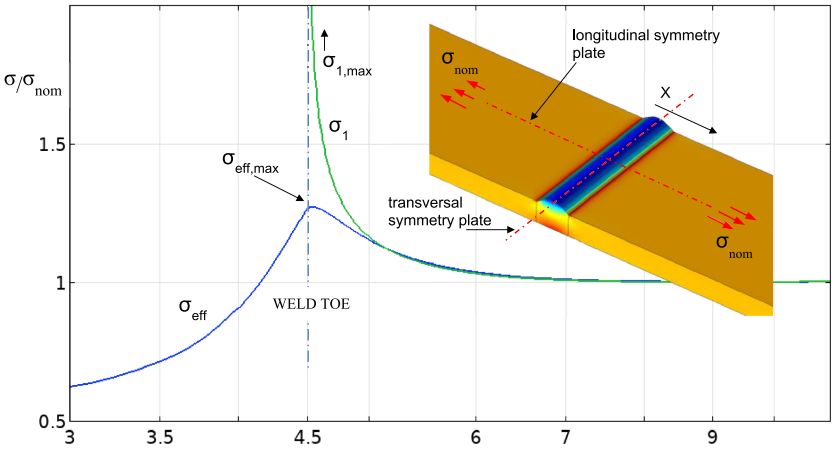

FIGURE 2 Effective stress in dimensionless form along the longitudinal symmetry plane for the butt-welded joint in Figure 1. x is zero at the transversal symmetry plane. [Colour figure can be viewed at wileyonlinelibrary.com]

gives more relevance, in the average process, to points around $\boldsymbol{P}$.

In this paper, Equation 1 was numerically solved by means of COMSOL Multiphysics software with quadratic elements. In general, in the critical zone, the mesh must have a minimum size around c,[26] and a free mesh generator with tetrahedral elements can be used.

With regard to the fatigue assessment, the ratio between the maximum effective stress $\sigma_{eff,max}$ and the nominal stress can be directly defined as the fatigue strength reduction factor K_f:

$$K_f = \frac{\sigma_{eff,max}}{\sigma_{nom}} \tag{3}$$

Figures 1 and 2 show the effective stress in a butt-welded joint. The main plate thickness of the butt weld is equal to 6 mm, the tensile loading is applied at the remote

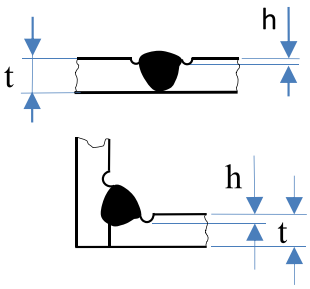

FIGURE 3 Typical undercut shape reported in the ISO documents [Colour figure can be viewed at wileyonlinelibrary.com]

nominal section, and the weld toe radius is set equal to zero. The dimensions of the joints are reported in Figure 1 as well as the effective stress with a color scale. In this example, the maximum effective stress at the weld toe is on the longitudinal symmetry plane. Despite the

14602695, 2022, 11, Downloaded from https://onlinelibrary.wiley.com/doi/10.1111/ffe.13812 by Universita Di Ferrara, Wiley Online Library on [20/06/2024]. See the Terms and Conditions (https://onlinelibrary.wiley.com/terms-and-conditions) on Wiley Online Library for rules of use; OA articles are governed by the applicable Creative Commons License

first principal stress σ_1 becoming singular at the weld toe, the effective stress σ_{eff} assumes a finite value, and this allows us to directly use the effective stress as a fatigue parameter.

2 | NUMERICAL ANALYSIS OF UNDERCUTS

Undercuts are frequent imperfections causing a decrease in durability of the welded joint. They are located close to or at weld toes and can have different shapes and dimensions. The technical documents in the literature often describe the shape of the undercuts approximately. In the reference figure given in the ISO documents, the undercuts appear as rounded V-notches at the weld toe. Figure 3 shows an example of a typical shape. Hobbacher[4] gives some simple geometrical rules for defining the maximum depth of the undercut with reference to the main plate thickness. Table 1 reports the ratio of the allowable h/t for the undercut.

TABLE 1 Acceptance levels for weld toe undercuts in steel[4]

	Allowable undercut (h/t)	
Fatigue class	**Butt welds**	**Fillet welds**
100	0.025	Not applicable
90	0.05	Not applicable
80	0.075	0.05
71	0.10	0.075
63	0.10	0.10
56 and lower	0.10	0.10

[a]Undercut deeper than 1 mm shall be assessed as a crack-like imperfection.
[b]The table is only applicable for plate thicknesses from 10 to 20 mm.

In order to underline that the actual undercut shape plays an important role in the definition of the effective K_f, in this section, some undercuts, either theoretically assumed or real, will be taken into account in the following, with modifications compared to the simple geometrical shape. The reference welded joints are full penetration cruciform joints. The considered undercuts will be set at the weld toe, similar to Figure 3. The first set of considered geometries are theoretically defined, similarly to that of Figure 3, but with a shape generally classifiable as cylindrical or spherical.

Figure 4 gives the considered spherical and cylindrical undercuts with different diameter values. The cylindrical undercut has a given radius of the cylinder and a variable depth. These theoretical geometrical features can be referred or turning out from as erroneous mark grinding or from an incorrect general welding technique and gas porosity.

The cylindrical undercut appears more critical than the spherical one in terms of maximum effective stress $\sigma_{eff,max}$. This criticality is mainly related to the sharpness of the edges; regardless of the theoretically infinite linear elastic stress concentration factor, the investigation provides a finite effective stress assessment. The presence of undercut increases the K_f, and this means a reduction in fatigue strength. The advantage of the implicit gradient approach is that the effective stress is directly correlated to the fatigue strength of the joints without any further post-processing elaboration (see next section) that can be time consuming.

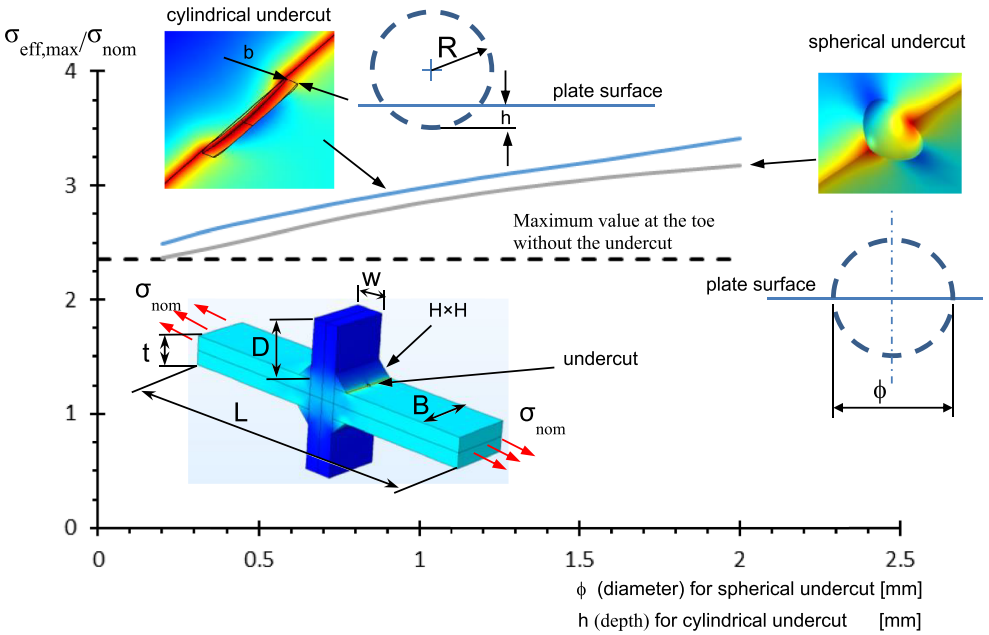

FIGURE 4 Effective stress in dimensionless form for the full penetration cruciform joint (t = 20 mm; H = 10 mm, W = 20 mm, L = 220 mm, B = 40 mm, D = 40 mm, R = 50 mm with fillet radius equal to R/300, b = 1 mm). The undercut is located at the weld toe and on the longitudinal symmetry axis. [Colour figure can be viewed at wileyonlinelibrary.com]

14602695, 2022, 11, Downloaded from https://onlinelibrary.wiley.com/doi/10.1111/ffe.13812 by Universita Di Ferrara, Wiley Online Library on [20/06/2024]. See the Terms and Conditions (https://onlinelibrary.wiley.com/terms-and-conditions) on Wiley Online Library for rules of use; OA articles are governed by the applicable Creative Commons License

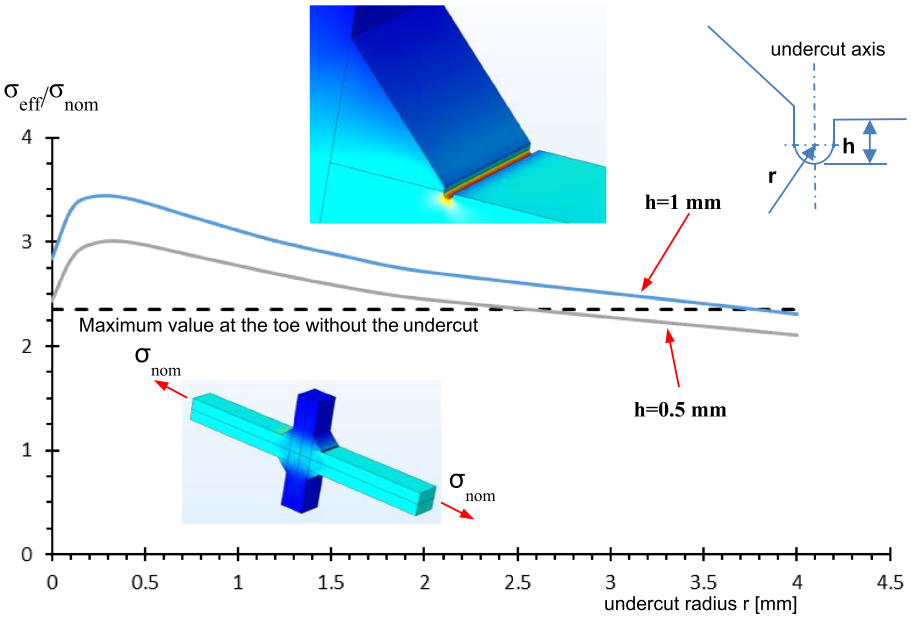

FIGURE 5 Effective stress in dimensionless form for the full penetration cruciform joint with a continuous undercut (t = 20 mm; H = 10 mm, W = 20 mm, L = 220 mm, B = 40 mm, D = 40 mm, see Figure 4). The axis of the undercut is located at the weld toe. [Colour figure can be viewed at wileyonlinelibrary.com]

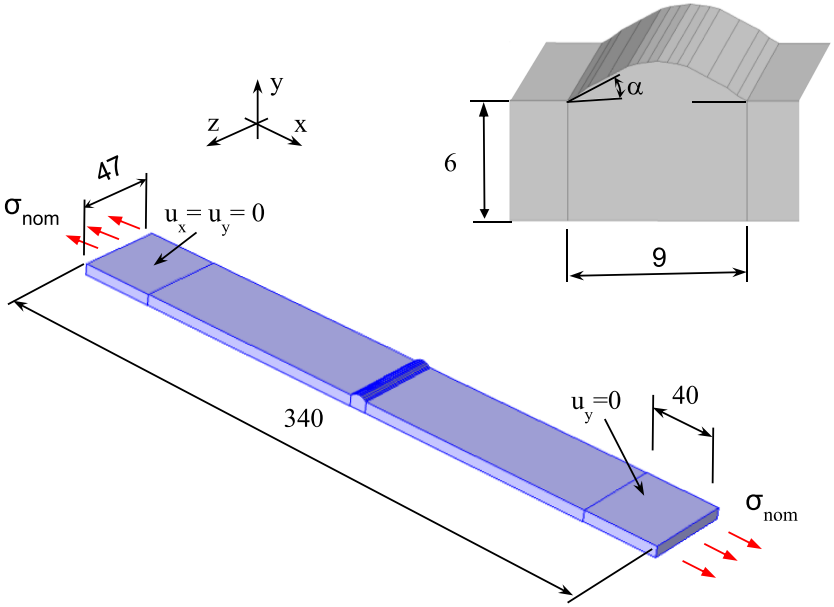

FIGURE 6 Geometry of the butt-welded joint under axial loading σ_{nom}[34] (dimension in millimeters; α = 30°) [Colour figure can be viewed at wileyonlinelibrary.com]

For a general comparison, Figure 5 shows the effective stress when the undercut is continuous with a rounded U-shape. The undercut is kept at a constant depth equal to one or half a millimeter. The presence of the undercut increases the value of the effective stress in the weld provided that the notch radius is less than 2.5 mm for a depth of 0.5 and 3.7 mm for a depth of 1 mm. This means that the toe grinding technique can give an advantage if the radius of the burr is large enough. In fact, for an undercut with a depth of about 0.8 mm, a burr of 10 mm in diameter was used.[27]

More generally, the comparison of the figures gives an example of the influence of the initially assumed shape on the assessment of the influence each parameter has on strength in defected joints.

3 | FATIGUE LIFE IN WELDED JOINTS WITH UNDERCUTS

The relevance of the undercut in fatigue life performance has been underlined in many papers.[28–30]

In a previous work, the experimental fatigue strength of welded joints with pores was considered[31] in terms of the implicit gradient approach by correlating the fatigue life to the maximum effective stress $\sigma_{eff,max}$. Also, in the case of undercuts, the implicit gradient approach can be used without modifying the previous proposed procedure.[16]

The undercut, as well as the shape of the welded joints, can be measured with high accuracy by means of the optical 3D surface measurement device.[32–34] In

14602695, 2022, 11, Downloaded from https://onlinelibrary.wiley.com/doi/10.1111/ffe.13812 by Universita Di Ferrara, Wiley Online Library on [20/06/2024]. See the Terms and Conditions (https://onlinelibrary.wiley.com/terms-and-conditions) on Wiley Online Library for rules of use; OA articles are governed by the applicable Creative Commons License

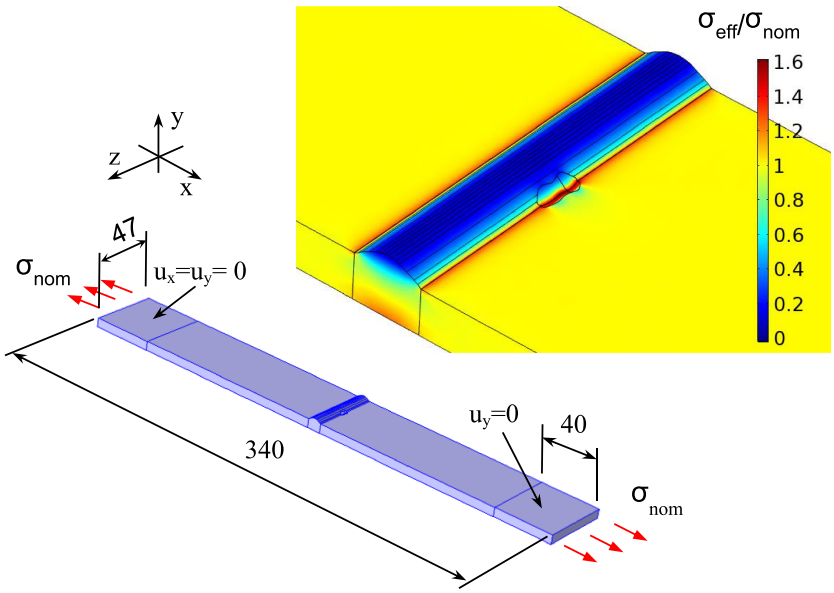

FIGURE 7 Effective stress in dimensionless form for butt-welded joint with an undercut under axial loading σ_{nom} (u displacement, dimension in millimeters) [Colour figure can be viewed at wileyonlinelibrary.com]

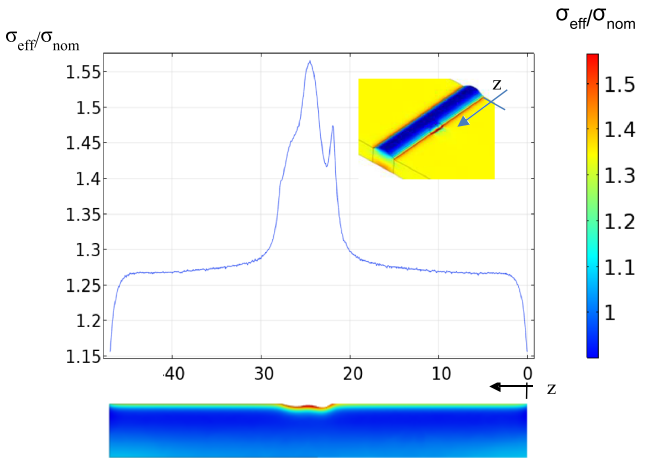

FIGURE 8 Effective stress in dimensionless form of the butt-welded joint of Figure 7 under axial loading σ_{nom} [Colour figure can be viewed at wileyonlinelibrary.com]

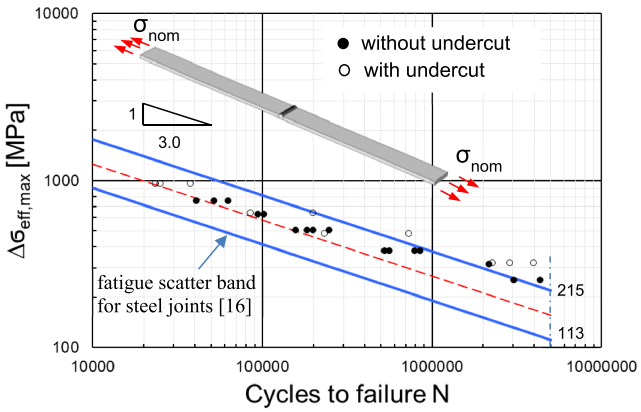

FIGURE 9 Range of maximum effective stress for a butt-welded joint of Figure 6 with and without an undercut under remote uniform tensile loading σ_{nom} (nominal load ratio equal to 0.1, scatter bands related to mean values plus/minus 2 standard deviations) [Colour figure can be viewed at wileyonlinelibrary.com]

particular, Ottersböck et al.[34] measured the weld with a minimum measurable radius of 20 μm. Furthermore, the paper included useful graphs and pictures to rebuild the typical undercut shape in the butt-welded joints made of ultra-high strength steel S1100 with a thickness of 6 mm. In order to produce small individual undercuts, the welding process parameters knowingly deviate from the optimum process settings.[34]

Figure 6 reports the geometry analyzed in Ottersböck et al.[34] where it was assumed that the reinforcement angle α was equal to 30° (the average reinforcement angle is about 25 to 30°, and the undercut exhibits a significantly steeper angle of nearly 40°). The length of the specimen was assumed according to Ottersböck et al.,[35] and the boundary conditions used in the present FE analysis are reported in Figure 6. Figure 7 proposes a rebuilding of the typical undercut analyzed in Ottersböck et al.[34] The length is about 6 mm with a maximum depth of about 0.4 mm. The effective stress is show in Figure 8 along the transversal cross section of the weld at the toe. The increasing effective stress is clear. The maximum is inside the undercut, and $\sigma_{eff,max}/\sigma_{nom}$ reaches the value of about 1.6 in contrast to 1.3 obtained without the undercut.

Finally, Figure 9 reports the fatigue data in terms of maximum effective stress $\sigma_{eff,max}$ by assuming specimens with undercut as in Figure 7. In Figure 9, the fatigue scatter band is related to mean values plus/minus 2 standard deviations. The agreement is satisfactory. Note that despite the

14602695, 2022, 11, Downloaded from https://onlinelibrary.wiley.com/doi/10.1111/ffe.13812 by Universita Di Ferrara, Wiley Online Library on [20/06/2024]. See the Terms and Conditions (https://onlinelibrary.wiley.com/terms-and-conditions) on Wiley Online Library for rules of use; OA articles are governed by the applicable Creative Commons License

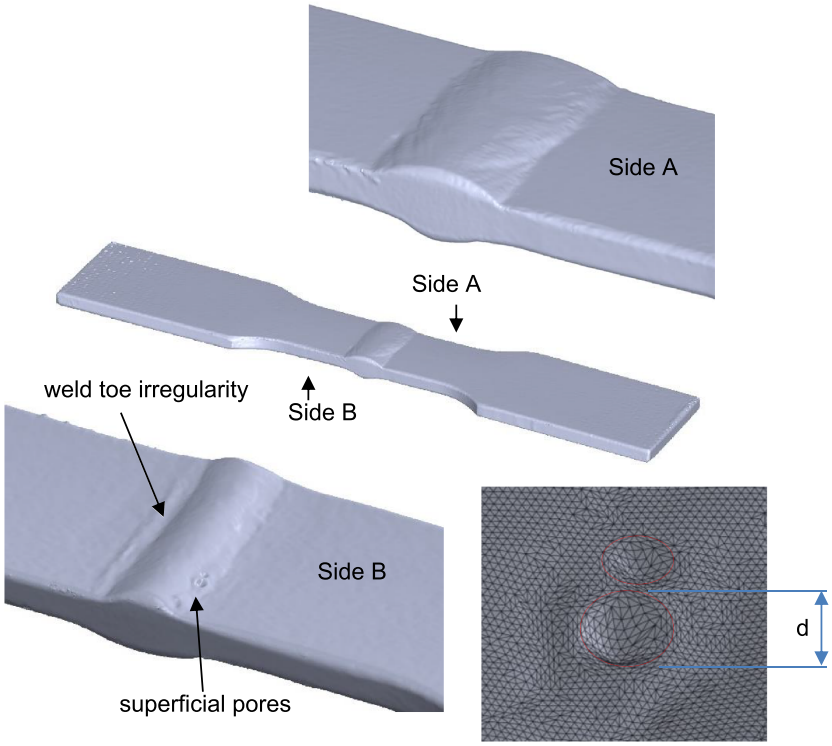

FIGURE 10 Three-dimensional model of a butt-welded joint obtained with a scanner resolution of about 0.1 mm (size of specimen 168 × 30 × 3 mm; d ∼ 1 mm) [Colour figure can be viewed at wileyonlinelibrary.com]

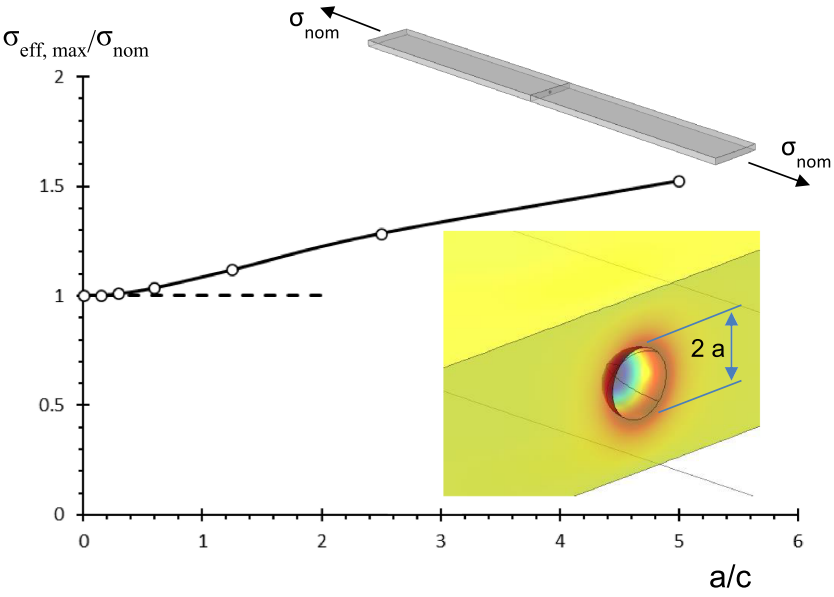

FIGURE 11 Maximum effective stress in dimensionless form for a plate with a spherical defect in the middle (size of specimen: length 400 mm; width 40 mm, thickness 5 mm; $c = 0.2$ mm) [Colour figure can be viewed at wileyonlinelibrary.com]

high static performance of the steel,[34] the fatigue behavior after the weld process is similar to other types of construction steel.[16,36]

4 | FE ANALYSIS FROM A THREE-DIMENSIONAL SCAN

The ISO 5817:2014 takes into account the quality levels of imperfections in fusion-welded joints and classifies the flaw in different categories. However, the reference figures are from a two-dimensional reference system, and the shape of the reference imperfections therefore needs to be given in a simplified form. A limit for imperfections is given for the three categories: B, C, and D. For the sake of simplicity, in the scientific literature, defects are usually considered in two-dimensional models where the average value of the characteristic geometry is used after an extensive experimental investigation.[34,35,37–39]

14602695, 2022, 11, Downloaded from https://onlinelibrary.wiley.com/doi/10.1111/ffe.13812 by Universita Di Ferrara, Wiley Online Library on [20/06/2024]. See the Terms and Conditions (https://onlinelibrary.wiley.com/terms-and-conditions) on Wiley Online Library for rules of use; OA articles are governed by the applicable Creative Commons License

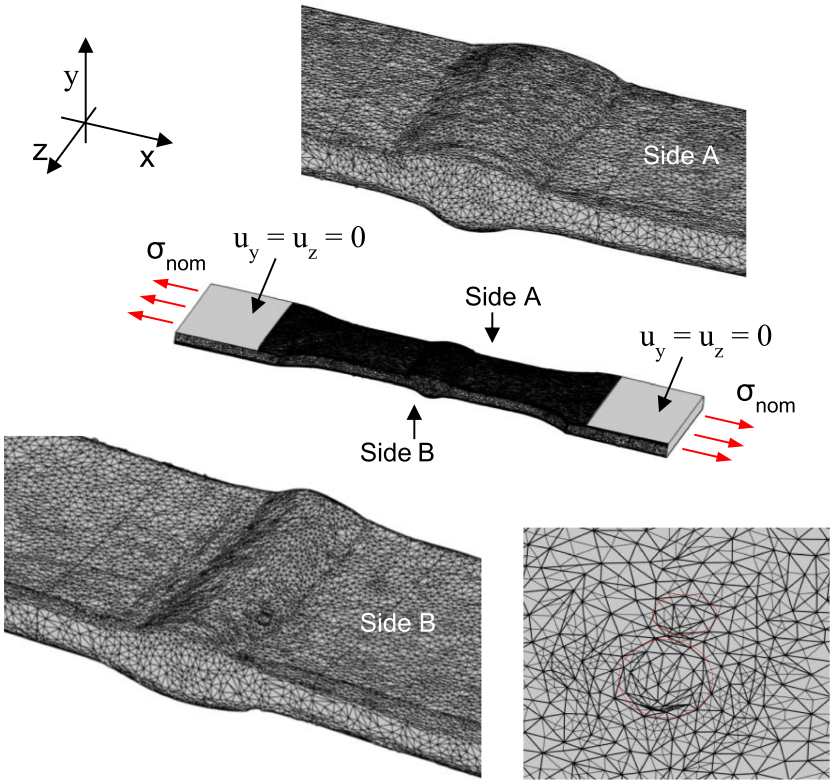

FIGURE 12 FE three-dimensional model used in the implicit gradient approach under a tensile nominal stress (mesh with minimum size of around 0.2 mm) [Colour figure can be viewed at wileyonlinelibrary.com]

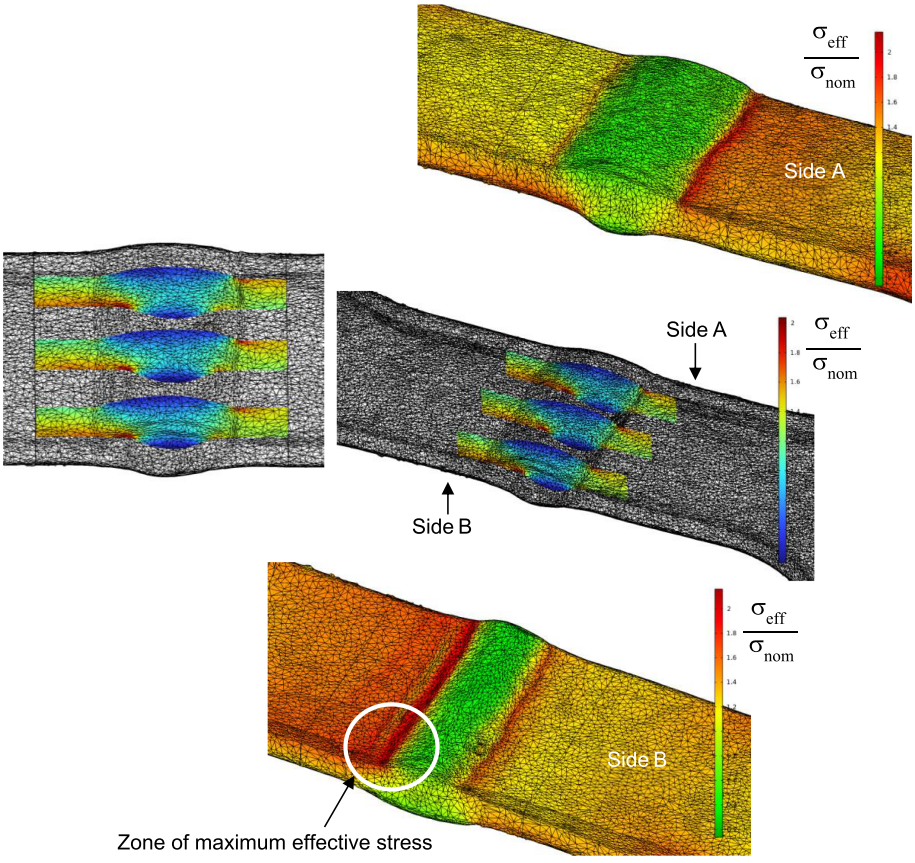

FIGURE 13 Effective stress obtained with the FE model of Figure 12. The maximum of effective stress is on side *B* where there is weld toe irregularity. [Colour figure can be viewed at wileyonlinelibrary.com]

14602695, 2022, 11, Downloaded from https://onlinelibrary.wiley.com/doi/10.1111/ffe.13812 by Universita Di Ferrara, Wiley Online Library on [20/06/2024]. See the Terms and Conditions (https://onlinelibrary.wiley.com/terms-and-conditions) on Wiley Online Library for rules of use; OA articles are governed by the applicable Creative Commons License

As suggested by ISO 5817, the schematic defects may be used in conjunction with a catalogue of realistic illustrations showing the size of the permissible imperfections for the various quality levels, by means of photographs showing the face and root side and/or reproductions of radiographs and photomacrographs showing the cross-section of the weld. According to this standard, an FE analysis based on a three-dimensional scan of the joints could be useful for capturing the effects of the actual weld shape[10,40,41] and also for considering superficial defects that are not classified in ISO 5817. In particular, the advantage given by the implicit gradient approach with a three-dimensional model is in its use of the same method given for welded structures analyzed without defects. Furthermore, the position of the maximum effective stress suggests the position of the crack growth initiation without any further post-processing operations.[16] Figure 10 reports a detailed three-dimensional model of a butt-welded joints obtained with a scanner Romer model 7320SI (by Hexagon Metrology, North Kingstown, USA). It has an accuracy of around 0.06 mm, and according to such value, the reliable three-dimensional surface shows many irregularities. In order to reproduce a correct three-dimensional model, it is sufficient that the scan resolution value is less than the material parameter c because the process zone, via the weight function introduced in Equation 2, is of the same order of magnitude of c. In general, if the scanner resolution is small in comparison to c, the local geometrical raiser does not substantially influence the effective stress as shown in Figure 11. When the diameter of the sphere is small in comparison to c, the maximum effective stress around the stress raiser tends to the tensile nominal stress so that the increment in effective stress can be negligible.

By using a scan resolution about 0.1 mm, the three-dimensional model of Figure 12 was obtained. On side B of the specimen, there are some superficial pores and weld toe irregularity. The butt-welded joint has been obtained from a tube so that the external surfaces in the central zone of the specimen are cylindrical. On the contrary, in the enlarged zone, the final shape appears flat after the specimen was clamped on the fatigue machine. By means of the virtual model of Figure 12, many types of defects can be take into account at the same time, such as an undercut, angular distortions, misalignments, and other types of defects.[3] Figure 13 reports the FE three-dimensional model used in the implicit approach under a tensile nominal stress with boundary conditions that prevent the rotation of the nominal section. Finally, the finite element analysis shows that the maximum effective stress is on side *B* where there is weld toe irregularity (see Figure 13). On the contrary, where superficial pores are detected, the stress concentration appears not to be critical.

5 | CONCLUSIONS

The implicit gradient approach gives us a practical tool for a parametric FE analysis of welded joints in a two-dimensional space as well as with three-dimensional models. The fatigue life is obtained without any other post-processing analysis.

By means of the implicit gradient approach, the actual geometry obtained by a three-dimensional scan of the welded joint can be directly used in the FE model without introducing any modifications. A 3D-scanned geometry can reproduce many types of defects at the same time, and then, by means of proper boundary conditions, the three-dimensional model can be examined in terms of effective stress. In order to avoid time consuming in numerical processes in reproducing the model, it is sufficient to have scanner accuracy comparable with the characteristic length of the material as well as the minimum size of the mesh in the FE model. The mesh can be generated with a free mesh generator with tetrahedral elements.

In the light of new technology, the implicit gradient approach is able to analyze each fillet weld for the evaluation of critical defects for a fatigue loading. In general, the presence of an undercut at the weld toe increases the stress concentration in terms of equivalent stress while decreasing the fatigue strength. However, in the case of an extensive radius of curvature with respect to the undercut depth, the fatigue stress reduction factor could increase.

DATA AVAILABILITY STATEMENT

Research data are not shared.

NOMENCLATURE

a	size of defects
B	width of the plate
c	characteristic length
D	length of secondary plate
E	elastic modulus
ϕ	diameter of spherical undercut
h	undercut size
H	weld leg size
K_f	fatigue strength reduction factor
L	length of the plate
n	outward normal vector
N	fatigue life; cycles to failure
ν	Poisson's ratio
r	notch radius
R	fillet radius
σ_1	first principal stress
σ_{nom}	nominal stress

14602695, 2022, 11, Downloaded from https://onlinelibrary.wiley.com/doi/10.1111/ffe.13812 by Universita Di Ferrara, Wiley Online Library on [20/06/2024]. See the Terms and Conditions (https://onlinelibrary.wiley.com/terms-and-conditions) on Wiley Online Library for rules of use; OA articles are governed by the applicable Creative Commons License

σ_{eff}	effective stress
$\sigma_{eff,max}$	maximum effective stress
σ_{eq}	equivalent stress
t	thickness
u	displacement
W	thickness of secondary plate
Ψ	weight function
Δ	range
∇^2	Laplace operator
∇	gradient

ORCID

Paolo Livieri https://orcid.org/0000-0002-1639-8928
Roberto Tovo https://orcid.org/0000-0002-9822-2730

REFERENCES

1. UNI EN 26520 (ISO 6520:1982), Classification of imperfections in metallic fusion welds.
2. ISO 5817:2014 Welding - Fusion-welded joints in steel, nickel, titanium and their alloys (beam welding excluded) - Quality levels for imperfections.
3. ISO 10042:2018 Welding -- Arc-welded joints in aluminium and its alloys -- Quality levels for imperfections.
4. Hobbacher A. *Recommendations for fatigue design of welded joints and components*. Paris, IIW: International Institute of Welding; 2007 *document* XIII-1823e07/XV-1254-07.
5. Schork B, Zerbst U, Kiyak M, Kaffenberger M, Madia MO, Oechsner M. Effect of the parameters of weld toe geometry on the FAT class as obtained by means of fracture mechanics-based simulations. *Weld World*. 2020;64(6):925-936. doi:10.1007/s40194-020-00874-7
6. VOLVO Standard STD 181-0004. Volvo Group Weld Quality Standard, 2008.
7. Remes H, Gallo P, Jelovica J, Romanoff J, Lehto P. Fatigue strength modelling of high-performing welded joints. *Int J Fatigue*. 2020;135:105555. doi:10.1016/j.ijfatigue.2020.105555
8. Jonsson B, Samuelsson J, Marquis GB. Development of weld quality criteria based on fatigue performance. *weld World*. 2011;55(11-12):79-88.
9. Livieri P, Tovo R. Analysis of the thickness effect in thin steel welded structures under uniaxial fatigue loading. *Int J Fatigue*. 2017;101:363-370.
10. Livieri P, Tovo R. The effect of throat underflushing on the fatigue strength of fillet weldments. *Fatigue Fract Eng Mater Struct*. 2013;36(9):884-892.
11. Bell R, Vosikovsky O, Bain SA. The significance of weld toe undercuts in the fatigue of steel plate T-joints. *Int J Fatigue*. 1989;11(1):3-11.
12. Zerbs UT, Schödel M, Webster S, Ainsworth R. *Fitness-for-service fracture assessment of structures containing cracks:* A workbook based on the European SINTAP/FITNET procedure. 1sted. Oxford Amsterdam the Netherlands: Elsevier; 2007.
13. Miki C, Fahimuddin F, Anami K. Fatigue performance of butt-welded joints containing various embedded defects. *Doboku Gakkai Ronbunshu*. 2001;2001(668):29-41.
14. BS 7910:2005. Guide to methods for assessing the acceptability of flaws in metallic structures
15. Fomin F, Horstmann M, Huber N, Kashaev N. Probabilistic fatigue-life assessment model for laser-welded Ti-6Al-4V butt joints in the high-cycle fatigue regime. *Int J Fatigue*. 2018;116:22-35.
16. Tovo R, Livieri P. An implicit gradient application to fatigue of sharp notches and weldments. *Eng Fract Mech*. 2007;74(4):515-526.
17. Livieri P, Tovo R. Fatigue strength of aluminium welded joints by a non-local approach. *Int J Fatigue*. 2021;143:106000.
18. Livieri P, Salvati E, Tovo R. A non-linear model for the fatigue assessment of notched components under fatigue loadings. *Int J Fatigue*. 2016;82(3):624-633.
19. Peerlings RHJ, de Borst R, Brekelmans WAM, de Vree JHP. Gradient enhanced damage for quasi-brittle material. *Int J Numer Methods Eng*. 1996;39(19):3391-3403.
20. Radaj D, Sonsino CM, Fricke W. *Fatigue assessment of welded joints by local approaches*. 2nded. Cambridge: Woodhead Publishing; 2006.
21. Pijaudier-Cabot G, Bažant ZP. Nonlocal damage theory. *J Eng Mech*. 1987;10:1512-1533.
22. Bažant ZP. Imbrigate continuum and its variational derivation. *J Eng Mech*. 1984;110(12):1693-1712.
23. Peerlings RHJ, Geers MGD, de Borst R, Brekelmans WAM. A critical comparison of nonlocal and gradient-enhanced softening continua. *Int J Solids Struct*. 2001;38(44-45):7723-7746.
24. Tovo R, Livieri P. An implicit gradient application to fatigue of complex structures. *Eng Fract Mech*. 2008;75(7):1804-1814.
25. Maggiolini E, Livieri P, Tovo R. Implicit gradient and integral average effective stresses: Relationships and numerical approximations. *Fatigue Fract Eng Mater Struct*. 2015;38(2):190-199.
26. Tovo R, Livieri P. A numerical approach to fatigue assessment of spot weld joints. *Fatigue Fract Eng Mater Struct*. 2011;34(1):32-45.
27. Zhang YH, Maddox SJ. Fatigue life prediction for toe ground welded joints. *Int J Fatigue*. 2009;31(7):1124-1136.
28. Janosch JJ, Debiez S. Influence of the shape of undercut on the fatigue strength of fillet welded assemblies-application of the local approach. *weld World*. 1998;41(2):350-360.
29. Cerit M, Kokumer O, Genel K. Stress concentration effects of undercut defect and reinforcement metal in butt welded joint. *Eng Fail Anal*. 2010;17(2):571-578.
30. Nguyen NT, Wahab MA. The effect of undercut, misalignment and residual stresses on the fatigue behaviour of butt welded joints. *Fatigue Fract Eng Mater Struct*. 1996;19(6):769-778.
31. Livieri P, Tovo R. Influence of porosity on the fatigue behaviour of welded joints IOP Conf Ser: Mater Sci Eng 1038 012051 2021.
32. Shiozaki T, Yamaguchi N, Tamai Y, Hiramoto J, Ogawa K. Effect of weld toe geometry on fatigue life of lap fillet welded ultra-high strength steel joints. *Int J Fatigue*. 2018;116:409-420.
33. Hultgren G, Barsoum Z. Fatigue assessment in welded joints based on geometrical variations measured by laser scanning. *weld World*. 2020;64:1825-1831.
34. Ottersböck MJ, Leitner M, Stoschka M, Maurer W. Effect of Weld Defects on the Fatigue Strength of Ultra High-Strength Steels *XVIII International Colloquium on Mechanical Fatigue of Metals (ICMFM XVIII). Proc Eng*. 2016;160:214-222.
35. Ottersböck MJ, Leitner M, Stoschka M, Maurer W. Analysis of fatigue notch effect due to axial misalignment for ultra high-strength steel butt joints. *Weld World*. 2019;63(3):851-865.

14602695, 2022, 11, Downloaded from https://onlinelibrary.wiley.com/doi/10.1111/ffe.13812 by Universita Di Ferrara, Wiley Online Library on [20/06/2024]. See the Terms and Conditions (https://onlinelibrary.wiley.com/terms-and-conditions) on Wiley Online Library for rules of use; OA articles are governed by the applicable Creative Commons License

36. Livieri P, Lazzarin P. Fatigue strength of steel and aluminium welded joints based on generalised stress intensity factors and local strain energy values. *Int J Fract*. 2005;133(3):247-376.
37. van Es SHJ, Kolstein MH, Pijpers RJM, Bijlaard FSK. TIG-dressing of high strength steel butt welded connections – part 1: weld toe geometry and local hardness. *Proc Eng*. 2013;66:216-225.
38. Lillemäe I, Remes H, Liinalampi S, Itävuo A. Influence of weld quality on the fatigue strength of thin normal and high strength steel butt joints. *Weld World*. 2016;60(4):731-740.
39. Nykänen T, Björk T, Laitinen R. Fatigue strength prediction of ultra high strength steel butt-welded joints. *Fatigue Fract Eng Mater Struct*. 2012;36(6):469-482.
40. Hou CY. Fatigue analysis of welded joints with the aid of real three-dimensional weld toe geometry. *Int J Fatigue*. 2007;29(4):772-785.
41. Pelizzari J, Maltauro M, Campagnolo A, Uccheddu F, Dengo C, Meneghetti G. Evaluation of the multi-axial fatigue resistance of stainless steel welded joints for automotive applications using the peak stress method (in Italian) 50th AIAS Congress, 1537 (19 pages). 2021.

How to cite this article: Livieri P, Tovo R. Actual weld profile fatigue performance by digital prototyping of defected and un-defected joints. *Fatigue Fract Eng Mater Struct*. 2022;45(11):3436-3446. doi:10.1111/ffe.13812

14602695, 2022, 11, Downloaded from https://onlinelibrary.wiley.com/doi/10.1111/ffe.13812 by Universita Di Ferrara, Wiley Online Library on [20/06/2024]. See the Terms and Conditions (https://onlinelibrary.wiley.com/terms-and-conditions) on Wiley Online Library for rules of use; OA articles are governed by the applicable Creative Commons License